

## Directed Beam of Excitons Produced by Stimulated Scattering

A. Mysyrowicz

*Laboratoire d'Optique Appliquée, Ecole Nationale Supérieure de Techniques Avancées, École Polytechnique, Palaiseau, France*

E. Benson and E. Fortin

*Physics Department, University of Ottawa, Ontario, Canada*

(Received 10 April 1996)

Amplification of a directed beam of excitons by stimulated scattering is observed in Cu<sub>2</sub>O at 2 K. It indicates that an excitoner, the radiationless excitonic counterpart of a laser, can be realized in semiconductors. [S0031-9007(96)00733-8]

PACS numbers: 71.35.Lk

It is well known that half-integer spin particles (fermions) obey the Pauli exclusion principle, which prevents multiple occupancy of a given quantum state. On the other hand, particles with integer spin (bosons) obey a reverse rule. Their scattering probability towards a state already occupied by other bosons is enhanced by a factor  $n + 1$ , where  $n$  is the occupation number of the final state. Under favorable conditions, this quantum "attraction" can become precipitous. Light amplification by stimulated emission of radiation (LASER) provides a unique example of this effect for massless Bose particles, the photons. However, amplification by stimulated emission is a much more general effect applying to any bosonic field including massive particles. The recent observation of Bose-Einstein condensation (BEC) of cold atoms has triggered an intense search for the discovery of stimulated emission of atoms [1–3]. Stimulated emission of atoms could thus lead to an "atomic field laser."

In this Letter, we report evidence for the stimulated emission (*without participation of radiation*) in a special case of massive Bose particles, optically inactive excitons in a semiconductor. In its spontaneous form, the basic exciton scattering process consists in the annihilation of an exciton of energy  $E_i$  and wave vector  $\mathbf{K}_i$ , the creation of an exciton ( $E_f, \mathbf{K}_f$ ), and the simultaneous emission (or absorption) of an acoustic phonon ( $\hbar\omega_q, \mathbf{q}$ ). It represents one step in a chain of scattering events after injection of hot excitons in an insulating crystal leading

to their energy relaxation and to the establishment of a quasithermodynamic equilibrium among the particles. Since we deal with a three body elementary process, the initial exciton ( $E_i, \mathbf{K}_i$ ) is coupled to a continuum of final states ( $E_f, \mathbf{K}_f; \hbar\omega_q, \mathbf{q}$ ), defined by the set of vectors ( $\mathbf{K}_f, \mathbf{q}$ ) which satisfy energy and momentum conservation laws:

$$E_i = E_f \pm \hbar\omega_q, \quad \mathbf{K}_i = \mathbf{K}_f \pm \mathbf{q}, \quad (1)$$

with the additional constraints

$$E_{i,f} = \frac{\hbar^2 K_{i,f}^2}{2m}, \quad \hbar\omega_q = \hbar\mathbf{q} \cdot \mathbf{v}, \quad (2)$$

where  $v$  is the longitudinal sound velocity in the crystal and  $m$  the exciton effective mass. From the point of view of excitonic motion, the succession of such spontaneous events leads to a diffusive exciton transport.

In the stimulated version of the process, exciton scattering is induced by an incident exciton field ( $n_c, E_c, \mathbf{K}_c$ ), where  $n_c \gg 1$  is the occupation number of mode  $c$ . The directions and magnitudes of  $\mathbf{K}_f$  and  $\mathbf{q}$  are prescribed by the supplementary conditions

$$\begin{aligned} E_f &= E_c, \\ \mathbf{K}_f &= \mathbf{K}_c. \end{aligned} \quad (3)$$

The growth of the bosonic wave is obtained from the time rate of change of the average number of bosons in mode  $c$  [4],

$$\begin{aligned} \frac{\partial n_c}{\partial t} &= \frac{2\pi}{\hbar} \sum_q \gamma^2(q) [n_{c+q}(1 + n_c) \{(1 + f_q)\delta(\hbar\omega_q + E_c - E_{c+q}) + f_q\delta(\hbar\omega_q - E_c + E_{c+q})\} \\ &\quad - n_c(1 + n_{c+q}) \{(1 + f_q)\delta(\hbar\omega_q - E_c + E_{c+q}) + f_q\delta(\hbar\omega_q + E_c - E_{c+q})\}], \end{aligned} \quad (4)$$

where  $n_i = n_{c+q}$  and  $f_k$  are, respectively, the occupation probabilities of excitons and acoustic phonons with energy  $E_k$  and  $\hbar\omega_k$ , and  $\gamma(q) = \gamma_0 \sqrt{q}$  is the matrix element of the exciton-phonon interaction. An excitonic Bose condensate with  $n_c \gg 1$  on the right-hand side of Eq. (4) can provide the triggering term for the stimulated excitonic transition. However, stimulated exciton scatter-

ing can occur even below Bose condensation threshold since in the quantum-degenerate statistical regime several exciton modes near  $K = 0$  have already a large occupation number. The first term in Eq. (4) expresses an amplification process; the second term a loss process in which an exciton is scattered out of mode  $n_c$  by the creation of an exciton of wave vector  $\mathbf{K}_c \pm \mathbf{q}$ . If stimulated

exciton emission overcomes induced exciton absorption, a net gain is achieved for the excitonic field. In the context of excitonic transport, stimulated exciton scattering induced by a traveling excitonic field ( $n_c, E_c, K_c$ ) leads to its amplification.

Experimental evidence for exciton amplification by stimulated exciton scattering is shown in Figs. 1(a) and 1(b). Consider first the lower traces. They display the time-resolved excitonic flux reaching the back surface of the sample immersed in superfluid He at 2 K after irradiation of the front surface with a laser pulse. The laser pulse has a duration of 10 ns and a peak intensity of  $63I_0$  where  $I_0 = 10^5 \text{ W/cm}^2$ ; the incident photons

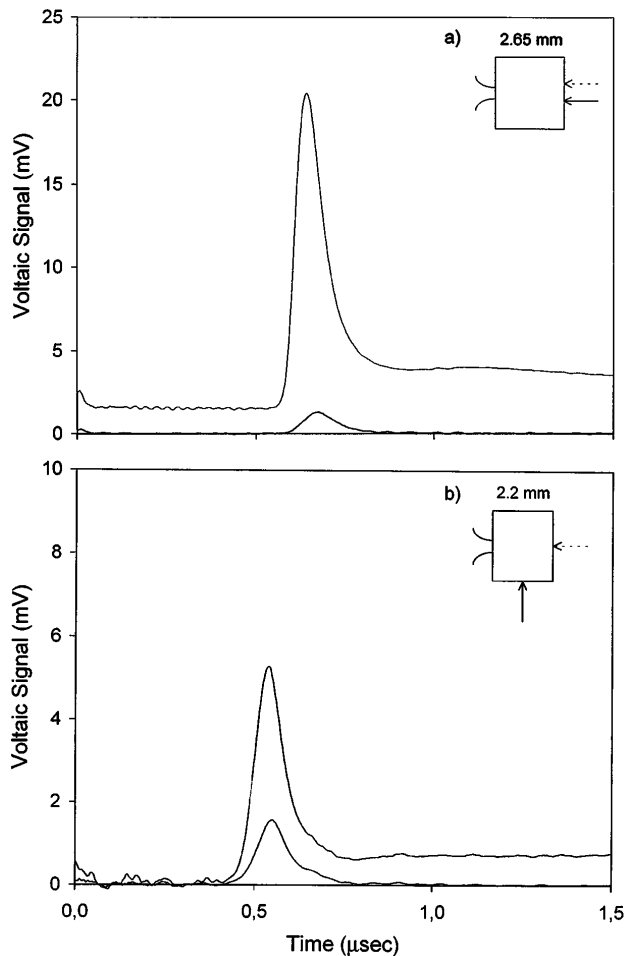


FIG. 1. (a) Collinear geometry: Voltaic signal obtained at the back surface of a 2.65 mm thick single crystal of  $\text{Cu}_2\text{O}$  held at  $T = 2 \text{ K}$ . The lower trace is obtained when the front sample surface is illuminated with a laser pulse ( $\lambda = 532 \text{ nm}$ ; duration 10 ns) of peak intensity  $I \approx 6.3 \text{ MW/cm}^2$ . The upper trace is the voltaic signal obtained under the same pulsed illumination while the sample front surface is illuminated with a cw laser of wavelength  $\lambda = 605.4 \text{ nm}$  and intensity  $I \approx 4 \text{ W/cm}^2$ . (Inset: solid arrow = cw laser; dashed arrow = pulsed laser; curved lines = wires to the oscilloscope.) (b) Orthogonal geometry: Same as (a) except that the pulsed laser intensity is  $50 \text{ kW/cm}^2$  and the cw laser is incident on a lateral face of a 2.2 mm thick sample.

( $\lambda = 532 \text{ nm}$ ) are absorbed within  $10 \mu\text{m}$  from the sample surface and converted into electron-hole pairs which themselves quickly form a mixture of hot  $n = 1$  orthoexcitons and paraexcitons. The hot excitons reach a temperature close to the lattice temperature within a few nanoseconds after the end of the optical pulse by cascade emission of optical and acoustic phonons. Orthoexcitons are known to down-convert into paraexcitons within tens of nanoseconds so that only “cold” paraexcitons survive at later times [5]. A pair of metallic films in the form of concentric rings (Au and Cu) deposited on the back surface acts as a local excitonic detector, via the exciton-mediated voltaic effect [6–8]. The built-in electric field at the copper-cuprous oxide interface is strong enough to dissociate excitons reaching the immediate vicinity of the back crystal surface. The liberated free holes are swept across the contact, while the corresponding electrons are collected through the gold Ohmic contact. It gives rise to an external voltaic signal in the absence of applied electric field which is measured across an external  $50 \Omega$  load resistance. This method of detecting excitons is well adapted to  $\text{Cu}_2\text{O}$ , because the excitons of lowest energy ( $n = 1$  paraexcitons) are not coupled to the radiation field and therefore are difficult to observe by optical means such as photoluminescence.

The voltaic responses shown in Fig. 1 correspond to a “packet” of excitons traveling together at a speed close to the sound velocity of the crystal ( $v_1 = 4.5 \times 10^5 \text{ cm/s}$ ). This peculiar mode of excitonic propagation is observed in  $\text{Cu}_2\text{O}$  instead of the normal diffusive behavior at high particle densities and sufficiently low crystal temperatures. It has been interpreted as evidence for an excitonic Bose condensate flowing ballistically through the crystal (excitonic superfluid) [7,8]. The slightly shorter transit time of the packet in Fig. 1(b) is accounted for by the smaller sample thickness  $d = 2.2 \text{ mm}$ .

The upper traces in Figs. 1(a) and 1(b) are obtained with the same pulsed excitation but now the sample is also illuminated with a cw dye laser tuned at  $\lambda = 605.4 \text{ nm}$ . The cw laser intensity is  $4 \text{ W/cm}^2$ . In Fig. 1(a), both lasers impinge on the front surface through an aperture 2 mm in diameter. In Fig. 1(b), the cw source illuminates a lateral sample surface through a diaphragm of 1 mm diameter. Absorption of the cw laser light occurs over a depth  $\alpha^{-1} \approx 0.3 \text{ mm}$  where  $\alpha$  is the absorption coefficient at  $\lambda = 605.4 \text{ nm}$ ; for each absorbed photon one orthoexciton is created with an initial kinetic energy of about 1.1 meV. The excitonic packet is now clearly amplified: While propagating, it has “attracted” excitons deposited deeper in the crystal by the cw laser beam.

The excitonic gain coefficient has been measured in the perpendicular geometry as a function of the cw laser intensity for two amplifier lengths. The amplifier length was changed by the use of a variable slit intercepting the path of the cw laser close to the sample. The results shown in Fig. 2 indicate an approximate linear

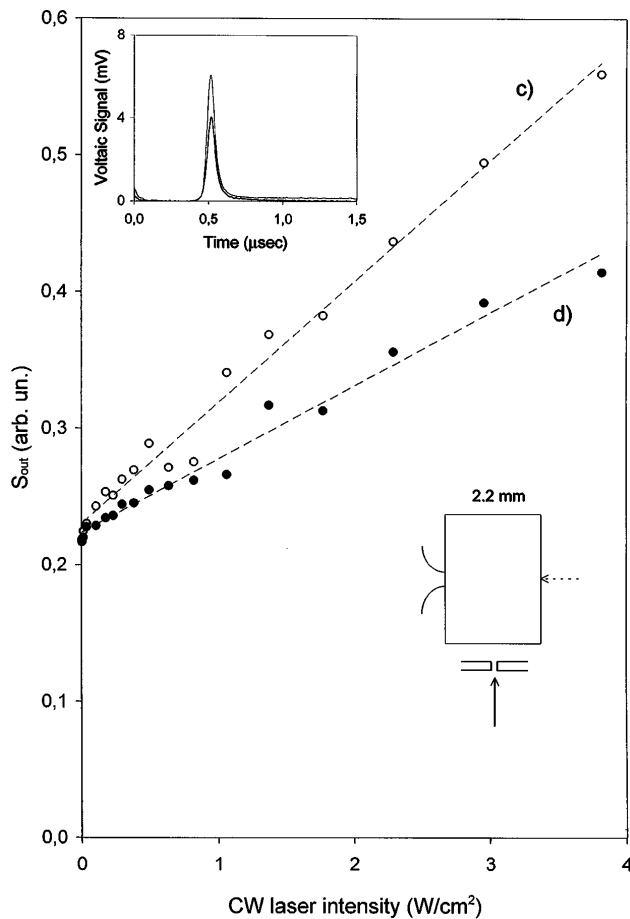


FIG. 2. Amplification  $G = S_{out}/S_{in}$  as a function of cw laser intensity (orthogonal geometry).  $S_{out}$  is the integral of the time-resolved voltaic signal between 0.4 and 0.56  $\mu$ sec.  $S_{in}$  (the same integral for pulsed laser illumination alone) is kept constant. The empty circles are for a slit width of 250  $\mu$ m; the filled circles for a 150  $\mu$ m slit. Inset: the bottom trace is obtained with pulsed laser illumination alone ( $I = 20I_0$ ), while the top trace is the result of the same pulsed plus cw laser illumination ( $I_{cw} = 2 \text{ W/cm}^2$  through a 250  $\mu$ m slit). The sample (thickness 2.2 mm) is held at 2 K.

dependence of the gain  $G = S_{out}/S_{in}$  with cw intensity and amplifier path length. Expressing the amplification as  $G = e^{gz}$  with  $g \approx aI_{cw}$ , where  $I_{cw}$  is the cw laser intensity and  $z$  the slit width, we obtain a gain coefficient  $a = 15 \text{ cm/W}$  for a large pulsed input  $I = 20I_0$ . Similar measurements performed with small input ( $I = 2I_0$ ) yield a larger gain coefficient  $a = 80 \text{ cm/W}$ . It indicates the presence of a saturation of the amplification.

The saturation of the gain is also seen in the collinear geometry. In Fig. 3, the difference between output and input signals  $S_{out} - S_{in} = S_{in}(G - 1)$  is plotted as a function of cw laser intensity for a small input signal  $I = 0.63I_0$ . The full line is a fit of the data with the following equation:

$$G - 1 = \frac{cI_{cw}}{(1 + I_{cw}/I_{sat})^{1/2}}, \quad (5)$$

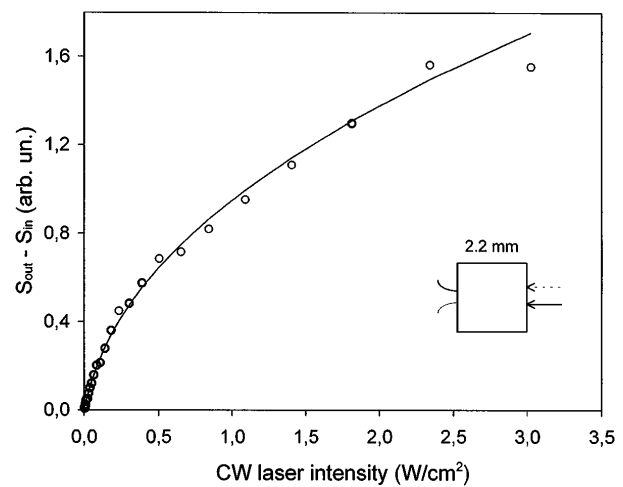


FIG. 3.  $S_{out} - S_{in} = G - 1$  as a function of cw laser intensity in the collinear geometry.  $S_{out}$  and  $S_{in}$  are defined in the caption of Fig. 2. The cw laser wavelength is  $\lambda = 605.4 \text{ nm}$ ; the pulsed laser has a peak intensity of  $0.63I_0$ . The solid line is a fit to the data with Eq. (5) introducing the following parameters:  $C = 0.2$ ,  $I_{sat} = 1.8 \text{ W/cm}^2$ . The sample thickness is 2.2 mm.

expressing again the presence of saturation as the signal becomes amplified. Similar saturation curves have been measured for larger input signal, but with a larger initial slope and a smaller value of  $I_{sat}$ .

We attribute the observed amplification of the excitonic packet to the stimulated emission of excitons into the packet. What is the origin of the macroscopic excitonic field ( $n_c, E_c, \mathbf{K}_c$ ) inducing the exciton transition? Since the pulsed laser creates hot free carriers which rapidly pair into excitons, a random distribution of particles in phase space exists initially near the sample front surface. The subsequent accumulation of a large number of particles in a single phase mode  $\mathbf{K}_c$  implies therefore a self-organization process. As discussed in recent papers [8,9], the onset conditions for ballistic propagation are in good agreement with the threshold conditions for a Bose-Einstein condensation of excitons. We believe this process provides the incident excitonic wave ( $n_c, E_c, \mathbf{K}_c$ ) stimulating the transition. There is natural explanation to the fact that the excitonic amplifier operates in the saturation limit: Above threshold for BEC, a substantial fraction of the total number of particles collect into one state, providing thereby a coherent bosonic field with a very large amplitude. One has therefore the situation of an amplifier with a large input signal where the rate of depletion of the pump exciton population by stimulated emission is significant compared to the rate of spontaneous emission.

As for a laser amplifier, system inversion must be realized in order to obtain excitonic gain. System inversion implies an irreversibility in the transfer of the excitons injected by the cw laser to the incident excitonic packet which in turn implies that these "pump" excitons are not

in thermal equilibrium with respect to the phonon thermal distribution [see Eq. (4)]. An off-equilibrium situation is realized in the present experiments because the pump orthoexcitons have an excess energy of at least  $\Delta E$  with respect to the condensed state, the paraexciton state at  $\mathbf{K}_c$ , where  $\Delta E = 12$  meV is the orthoexciton and paraexciton splitting.

Evidence for excitonic amplification is even more striking if the pulsed laser intensity is set below threshold for ballistic transport (see Fig. 4). The weak signal of long duration shown in the lower trace of the figure is characteristic of a diffusive transport regime with a large spread of particle transit times. This type of response can be well reproduced quantitatively with the continuity equation, using exciton diffusion constants from the literature [6,8]. The voltaic response obtained in the presence of both cw and pulsed laser in the collinear geometry displays the dramatic appearance of the ballistic packet (upper trace of Fig. 4). The amplification  $G$  is now orders of magnitude larger than in the case of Fig. 1, since the input signal ( $S_{in}$  at the time of arrival of the packet)

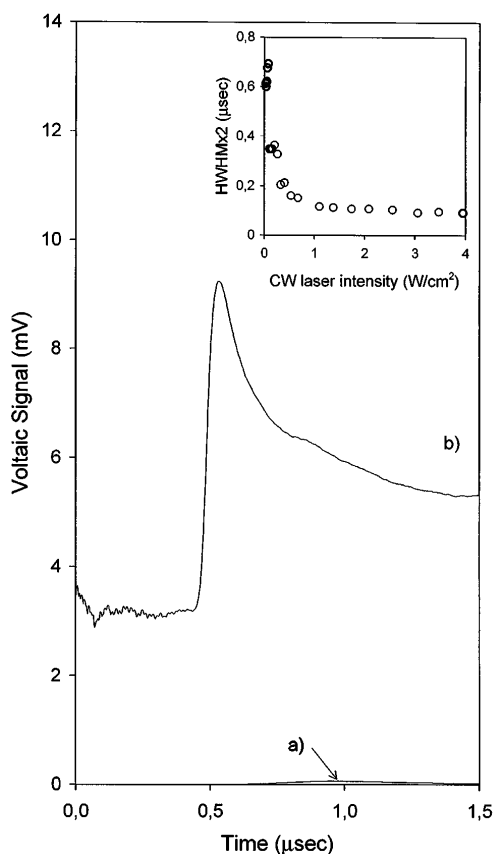


FIG. 4. Trace (a) shows the time-resolved signal obtained from pulsed illumination only with peak intensity  $I = 0.63I_0$ . Trace (b) is obtained by illumination with a cw laser of wavelength  $\lambda = 605.4$  nm and intensity  $I \approx 4$  W/cm<sup>2</sup> in addition to the same pulsed laser. In the inset twice the half width at half maximum of the leading edge of the signal is plotted as a function of cw laser intensity.

is very small. The transition from diffusive to coherent transport occurs over a small increase of the number of excitons. This is best seen by plotting the rise time of the voltaic signal as a function of cw laser intensity (inset of Fig. 4). The steep rise time of the voltaic response heralds the grouped arrival of the particles.

The results of Fig. 4 are particular in the sense that the excitons produced by each laser source separately are incoherent. The change from spontaneous (incoherent excitons with diffusive transport) to stimulated emission (coherent exciton field with collective ballistic transport) which takes place over an abrupt thresholdlike range of combined pumping conditions represents the excitonic analog of a single pass laser without external cavity. With an appropriate resonance cavity, a genuine radiationless multiple pass “excitonic laser” or excitoner with reduced pumping threshold should be realizable.

A question which has not been addressed here relates to the origin of the increased voltaic signal observed in Figs. 1, 2, and 4 after the passage of the amplified ballistic pulse. Under certain conditions of pump and input signals, this increased excitonic flux is followed at later times by an abrupt decrease below the steady-state level of excitonic current. This excitonic depletion is itself succeeded by a gradual recovery to the steady-state value. This points out a rich excitonic hydrodynamics, which will be reported in an upcoming presentation.

In conclusion, we have shown that amplification of a directed excitonic beam can be achieved by stimulated exciton scattering. The experimental observation of such an effect could lead to the better understanding of coherent transfer of energy or current in several physical systems.

We acknowledge the support of a NATO grant (CRG 940549) and a very useful discussion with Y. Castin, G. Grynberg, and C. Salomon.

- [1] M.H. Anderson, J.R. Ensher, M.R. Matthews, C.E. Wieman, and E.A. Cornell, *Science* **269**, 198 (1995).
- [2] C.C. Bradley, C.A. Sackett, J.J. Tollett, and R.G. Hulet, *Phys. Rev. Lett.* **75**, 1687 (1995).
- [3] K.B. Davis, M.-O. Mewses, M.R. Andrews, N.J. van Druten, D.S. Durfee, D.M. Kurn, and W. Ketterle, *Phys. Rev. Lett.* **75**, 3969 (1995).
- [4] E. Hanamura and H. Haug, *Phys. Rep. C* **33**, 209 (1977).
- [5] A. Mysyrowicz, D. Hulin, and A. Antonetti, *Phys. Rev. Lett.* **43**, 1123 (1979).
- [6] E. Tselepis, E. Fortin, and A. Mysyrowicz, *Phys. Rev. Lett.* **59**, 2107 (1987).
- [7] E. Fortin, S. Fafard, and A. Mysyrowicz, *Phys. Rev. Lett.* **70**, 3951 (1993).
- [8] E. Benson, E. Fortin, and A. Mysyrowicz, *Phys. Status Solidi B* **191**, 345 (1995).
- [9] D.W. Snoke, J.P. Wolfe and A. Mysyrowicz, *Phys. Rev. Lett.* **64**, 2543 (1990); J.-L. Lin and J.P. Wolfe, *Phys. Rev. Lett.* **71**, 1223 (1993).